



Published in final edited form as:

J Nat Prod. 2019 December 27; 82(12): 3469–3476. doi:10.1021/acs.jnatprod.9b01015.

Structure Determination, Functional Characterization, and Biosynthetic Implications of Nybomycin Metabolites from a Mining Reclamation Site-Associated *Streptomyces*

Xiachang Wang^{†,‡,§}, Sherif I. Elshahawi^{‡,§,⊥}, Larissa V. Ponomareva^{‡,§}, Qing Ye^{||}, Yang Liu^{‡,§}, Gregory C. Copley[∇], James C. Hower[∇], Bruce E. Hatcher[¶], Madan K. Kharel, Steven G. Van Lanen[§], Qing-Bai She^{||}, S. Randal Voss^{#,Δ,□}, Jon S. Thorson^{*,‡,§}, Khaled A. Shaaban^{*,‡,§}

[†]Jiangsu Key Laboratory for Functional Substances of Chinese Medicine, Nanjing University of Chinese Medicine, Nanjing 210023, People's Republic of China

[‡]Center for Pharmaceutical Research and Innovation, University of Kentucky, Lexington, Kentucky 40536, United States

[§]Department of Pharmaceutical Sciences, College of Pharmacy, University of Kentucky, Lexington, Kentucky 40536, United States

[⊥]Department of Biomedical and Pharmaceutical Sciences, Chapman University School of Pharmacy, Irvine, California 92618, United States

^{||}Markey Cancer Center, Department of Pharmacology and Nutritional Sciences, College of Medicine, University of Kentucky, Lexington, Kentucky 40536, United States

[∇]Center for Applied Energy Research, University of Kentucky, Lexington, Kentucky 40511, United States

[¶]Division of Water, Kentucky Energy and Environment Cabinet, 2642 Russellville Road, Bowling Green, Kentucky 42101, United States

School of Pharmacy, University of Maryland Eastern Shore, Princess Anne, Maryland 21853, United States

[#]Department of Neuroscience, University of Kentucky, Lexington, Kentucky 40536, United States

^ΔAmbystoma Genetic Stock Center, University of Kentucky, Lexington, Kentucky 40536, United States

[□]Spinal Cord and Brain Injury Research Center, University of Kentucky, Lexington, Kentucky 40536, United States

*Corresponding Authors: jsthorson@uky.edu.; khaled_shaaban@uky.edu.

Supporting Information

The Supporting Information is available free of charge at <https://pubs.acs.org/doi/10.1021/acs.jnatprod.9b01015>.

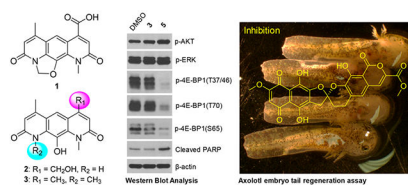
The workup isolation scheme, axolotl embryo tail regeneration assay figures treated with compounds 1–9, and full spectroscopic data (NMR and mass) of compounds 1–9 (PDF)

The authors declare the following competing financial interest(s): J.S.T. is a co-founder of Centrose (Madison, WI).

Abstract

We report the isolation and characterization of three new nybomycins (nybomycins B–D, **1–3**) and six known compounds (nybomycin, **4**; deoxynyboquinone, **5**; α -rubromycin, **6**; β -rubromycin, **7**; γ -rubromycin, **8**; and [2 α (1*E*,3*E*),4 β]-2-(1,3-pentadienyl)-4-piperidinol, **9**) from the Rock Creek (McCreary County, KY) underground coal mine acid reclamation site isolate *Streptomyces* sp. AD-3-6. Nybomycin D (**3**) and deoxynyboquinone (**5**) displayed moderate (**3**) to potent (**5**) cancer cell line cytotoxicity and displayed weak to moderate anti-Gram-(+) bacterial activity, whereas rubromycins **6–8** displayed little to no cancer cell line cytotoxicity but moderate to potent anti-Gram-(+) bacterial and antifungal activity. Assessment of the impact of **3** or **5** cancer cell line treatment on 4E-BP1 phosphorylation, a predictive marker of ROS-mediated control of cap-dependent translation, also revealed deoxynyboquinone (**5**)-mediated downstream inhibition of 4E-BP1p. Evaluation of **1–9** in a recently established axolotl embryo tail regeneration assay also highlighted the prototypical telomerase inhibitor γ -rubromycin (**8**) as a new inhibitor of tail regeneration. Cumulatively, this work highlights an alternative nybomycin production strain, a small set of new nybomycin metabolites, and previously unknown functions of rubromycins (antifungal activity and inhibition of tail regeneration) and also provides a basis for revision of the previously proposed nybomycin biosynthetic pathway.

Graphical Abstract



INTRODUCTION

Nybomycins are pyridoquinolinedione-based metabolites of *Streptomyces* isolated from diverse environments including terrestrial soil samples,^{1,2} marine sediments,^{3,4} and the body surface of carpenter ants.⁵ These secondary metabolites are selective inhibitors of a quinoline-resistant Ser84Leu mutant DNA gyrase (GyrA), and synthetic deoxynybomycin analogues display good oral bioavailability, tolerance, and efficacy in murine infection models.^{6–8} Conversely, the development of nybomycin resistance surprisingly resensitizes a bacterium to quinolone antibiotics, and thus, nybomycins have been designated as “reverse antibiotics”.^{6,8} Nybomycins are also active against both proliferating and dormant *Mycobacterium tuberculosis* the proposed mechanistic basis for which is GyrA-independent.³ In addition, some nybomycins display potent cancer cell line cytotoxicity where NAD(P)H quinone oxidoreductase 1 (NQO1)-mediated bioreductive activation and corresponding intracellular reactive oxygen species (ROS) production are believed to be the driving factors.^{9–14} Nybomycin analogues can also inhibit cell division cycle 25 (CDC25) phosphatases that serve as key regulators of the eukaryotic cell cycle and are highly overexpressed in many cancers.^{15,16} Despite these prominent diverse biological functions of nybomycins, corresponding biosynthetic studies are limited to early metabolic labeling studies^{17,18} and the more recent annotation of a nybomycin biosynthetic gene cluster,⁴ both implicating 4-

aminoanthranilic acid as a central progenitor. Given this context, access to new naturally occurring nybomycins, corresponding production strains, and/or their genomic-encoded biocatalysts may enable further probe/lead development and/or biosynthetic advances.

As part of an effort to discover new microbial natural products,^{19–28} their unique molecular targets,^{29,30} and/or corresponding biocatalysts,³¹ herein, we describe the isolation and structure elucidation of three new nybomycins (nybomycins B–D, **1–3**) and six previously reported metabolites (nybomycin, **4**; deoxynyboquinone, **5**; α -rubromycin, **6**; β -rubromycin, **7**; γ -rubromycin, **8**; and [2 α (1*E*,3*E*),4 β]-2-(1,3-pentadienyl)-4-piperidinol, **9**) from the Rock Creek (McCreary County, KY) underground coal mine acid reclamation site isolate *Streptomyces* sp. AD-3-6. Bioactivity studies revealed compounds **3** and **5** to afford moderate (**3**) to potent (**5**) cancer cell line cytotoxicity and weak to moderate anti-Gram-(+) bacterial activity. In contrast, the isolated rubromycins displayed little to no cancer cell line cytotoxicity but moderate to potent anti-Gram-(+) bacterial and antifungal activity. Consistent with **5**-mediated ROS production,⁹ and the recently established relationship between elevated [ROS] and the phosphorylation of the translational repressor 4E-BP1,^{29,30} **5** also inhibited phosphorylation of 4E-BP1. Using an axolotl embryo tail regeneration assay,^{25,27,30,32,33} evaluation of the set of isolated metabolites also identified **8** as an inhibitor of tail regeneration. These cumulative studies highlight an alternative nybomycin production strain, a small set of new nybomycin metabolites, and previously unknown functions of rubromycins (antifungal activity and inhibition of tail regeneration). In addition, a revision of the previously proposed nybomycin biosynthetic pathway is put forth based on the new metabolites described.

RESULTS AND DISCUSSION

Six actinomycete strains were purified from a single soil sample collected near an acid mine reclamation site in McCreary County, Kentucky. Metabolic profiling of these strains implicated *Streptomyces* sp. AD-3-6 as capable of unique metabolite production based on an AntiBase 2017³⁴ database comparison. Scale-up fermentation (10 L) of *Streptomyces* sp. AD-3-6, followed by extraction, fractionation, and iterative chromatography (silica gel column chromatography, Sephadex LH-20 column chromatography and semipreparative C₁₈ HPLC), gave nybomycins B (**1**, yield = 1.5 mg/L), C (**2**, yield = 0.5 mg/L), and D (**3**, yield = 0.3 mg/L), nybomycin (**4**, yield = 2.5 mg/L), deoxynyboquinone (**5**, yield = 0.2 mg/L), α -rubromycin (**6**, yield = 0.2 mg/L), β -rubromycin (**7**, yield = 1.1 mg/L), γ -rubromycin (**8**, yield = 0.6 mg/L), and [2 α (1*E*,3*E*),4 β]-2-(1,3-pentadienyl)-4-piperidinol (**9**, yield = 0.6 mg/L) (Supporting Information, Scheme S1).

Structure Elucidation.

Compounds **1** (C₁₆H₁₂N₂O₅), **2** (C₁₅H₁₄N₂O₄), and **3** (C₁₆H₁₆N₂O₃) displayed UV–vis and NMR signatures consistent with previously reported nybomycins.^{1,2,7,9,35–37} ¹H NMR, ¹³C NMR, and HSQC data (Table 1) of **1** were consistent with the presence of 16 carbons, including two methyls [δ_{H} 4.01 (3H, s)/ δ_{C} 33.8 (CH₃-11), and δ_{H} 2.49 (3H, s)/ δ_{C} 16.2 (CH₃-13)], one methylene [δ_{H} 6.42 (2H, s)/ δ_{C} 86.8 (CH₂-14)], three sp² methines [δ_{H} 7.47 (1H, s)/ δ_{C} 122.5 (CH-3), δ_{H} 8.59 (1H, s)/ δ_{C} 116.7 (CH-5), and δ_{H} 6.78 (1H, s)/ δ_{C} 117.8

(CH-7)], seven sp^2 nonprotonated carbons [δ_C 140.2 (C-4), δ_C 118.8 (C-4a), δ_C 117.1 (C-5a), δ_C 155.0 (C-6), δ_C 130.9 (C-9a), δ_C 138.2 (C-10), and δ_C 124.7 (C-10a)], and three acid/amide carbonyls [δ_C 163.3 (C-2), δ_C 160.0 (C-8), and δ_C 169.0 (C-12)]. Key HMBC correlations [from CH₃-11 to C-2/C-10a, from CH₃-13 to C-5a/C-6, from H-3 to C-2/C-4/C-4a/C-11/C-12, from H-5 to C-4/C-4a/C-6/C-9a/C-10a, and from H-7 to C-5a/C-8/C-13] further highlighted the close structural relationship of **1** and nybomycin (**4**, a previously reported metabolite also produced by *Streptomyces* sp. AD-3-6)^{1,35} with structural divergence in the C-4 substitution (Chart 1). Specifically, in **1**, the prototypical nybomycin C-4 exocyclic CH₂OH has been replaced by a COOH, key support for which was the observed CH-3 (δ_H 7.47) to C-12 (δ_C 169.0) HMBC correlation. Thus, the structure of **1** was established as a new member of the nybomycin family and subsequently named nybomycin B.

Cumulative analysis of NMR data (Table 1) indicated both **2** and **3** also shared the pyrido[3,2-*g*]quinoline-2,8(1*H*,9*H*)-dione core common to **1** and **4**. Compound **2** was distinguished by the lack of the **4** dihydro-oxazole CH₂. In contrast, the C-4 and N-9 methyl substitutions were the sole differentiating features of **3** (supported by HMBC correlations from CH₃-9/CH₃-1 to C-8/C-2 and C-9a/C-10a, from CH-13/CH₃-12 to C-6/C-4, C-7/C-4, and C-5a/C-4a), indicating the similarity of ring A/C in compound **3** (Chart 1, Figure 1, Table 1). Metabolites **2** and **3** were thereby designated as new nybomycins C and D.

Comparison of the NMR and MS data with literature values established the remaining known compounds as nybomycin (**4**),³⁵ deoxynyboquinone (**5**),⁹ α -rubromycin (**6**),³⁸ β -rubromycin (**7**),³⁹ γ -rubromycin (**8**),⁴⁰ and [2 α (1*E*,3*E*),4 β]-2-(1,3-pentadienyl)-4-piperidinol (**9**).⁴¹

All isolated compounds (**1–9**) were evaluated in standard antibacterial, antifungal, and cancer cell line cytotoxicity assays (Table 2, Figure 2, and Supporting Information, Figure S2). Nybomycin D (**3**) and deoxynyboquinone (**5**) were the only two metabolites to display moderate (**3**) to potent (**5**) cancer cell line cytotoxicity [A549 (human non-small cell lung): EC₅₀ for **3** (15.17 μ M) and **5** (0.25, μ M); PC3 (human prostate): EC₅₀ for compounds **3** (1.14 μ M) and **5** (0.15 μ M)]. Subsequent evaluation of 4E-BP1 phosphorylation, a predictive marker of ROS-mediated effects,^{29,30} in HCT116 (human colorectal) cancer cells treated with 1 μ M **3** or **5** revealed selective inhibition of 4E-BP1p in the presence of **5** (Figure 3A). Nybomycins **3** and **5** also displayed weak to moderate anti-Gram-(+) bacterial activity. In contrast, rubromycins **6–8** displayed little to no cancer cell line cytotoxicity but moderate to potent anti-Gram-(+) bacterial and antifungal activity. Evaluation of all isolated metabolites **1–9** in our recently developed axolotl embryo tail regeneration assay^{25,27,30,32,33} also highlighted **8** as a new inhibitor of tail regeneration (Figure 3B and Supporting Information, Figure S3).

Discussion.

Including the new naturally occurring nybomycins B–D (**1–3**) reported herein, 21 naturally occurring metabolites reminiscent of pyridoquinolinedione-based nybomycins have been reported.³⁴ These include nybomycin (**4**, produced by *Streptomyces* sp.),^{1,2,35}

hydroxynybomycin (derived from *Streptomyces* sp. D57),⁴² deoxynybomycin (derived from *S. hyalinum* and marine *Streptomyces* sp. B8855),³⁷ deoxynyboquinone (derived from the deep-sea actinomycete *Pseudonocardia* sp. SCSIO 01299),^{9,43} and other closely related metabolites BE-12233 [produced by *Streptomyces* sp. BA-12233 (FERM P-10492)],⁴⁴ Sch-538415 (produced by *Streptomyces* sp.),^{45,46} pseudonocardians A–C (derived from the deep-sea actinomycete *Pseudonocardia* sp. SCSIO 01299),⁴³ diazaquinomycin A [also known as antibiotic OM 704A and NSC 626554; derived from *Streptomyces* sp. om-704-ka 333 (FERM-p 6520) and *Streptomyces* sp. GW48/1497],^{47–49} diazaquinomycin B (also known as antibiotic OM 704B and 9,10-dihydrodiazaquinomycin A; produced by *Streptomyces* sp. om-704),^{47,49} diazaquinomycins C–D (produced by *Streptomyces* sp. GW48/1497),⁴⁸ and diazaquinomycins E–G (produced by the marine-derived *Streptomyces* sp.).^{50–52} The current study extends this previous work with both additional insights regarding metabolite function and biosynthesis.

From a functional perspective, the current work offers the following two primary advances. First, although NAD(P)H quinone oxidoreductase 1 (NQO1)-mediated bioreductive activation of **5** and corresponding intracellular ROS production is well-precedented,⁹ this study is the first to demonstrate the corresponding effect of **5** on 4E-BP1 phosphorylation. The phosphorylation status of 4E-BP1 was recently implicated as a potential predictive marker in response to ROS-based anticancer agents^{29,30}. Dysregulation of cap-dependent translation through redundant phosphorylation of the translational repressor 4E-BP1 by multiple oncogenic pathways, such as PI3K/AKT/mTOR and RAS/RAF/MEK/ERK, is associated with malignant progression and therapeutic resistance^{53–60}. Compounds that induce H₂O₂ and/or ROS production, such as **5**, activate the peroxisome-bound tuberous sclerosis complex, which leads to subsequent inhibition of mTORC1-mediated 4E-BP1 phosphorylation and concomitant repression of cap-dependent translation and cancer cell/tumor growth^{29,61,62}. Second, this study is also the first to reveal γ -rubromycin (**8**) as an inhibitor of axolotl embryo tail regeneration. In addition to their ability to inhibit HIV reverse transcriptase,^{63–66} both β - and γ -rubromycin (**7** and **8**, respectively) are also prototypical inhibitors of telomerase^{63,66–69}. Telomerase function is a central player in regeneration, aging, and cancer, where inhibition of telomerase correlates with reduced pluripotency/plasticity, premature aging, and reduced lifespan in various models^{70–74}. Importantly, axolotl telomerase increases during axolotl neonate tail regeneration based on Western blotting.⁷⁵ Although additional mechanistic studies are lacking, the ability of **8** to inhibit axolotl embryo tail regeneration implicates **8** as new chemical biology tool to mechanistically interrogate this unique regenerative model further.

From a biosynthetic standpoint, the current work provides additional support for the biosynthetic pathway recently put forth by Luzhetsky et al. and implicates new potential enzymatic and/or chemical avenues for diversification of the **4** scaffold (Figure 4).⁴ The central pyridoquinolinedione core of nybomycin was previously proposed to derive from 4-aminoanthracilic acid followed by NybS-catalyzed N-1/9-dimethylation to generate **3**. The isolation of **3** from *Streptomyces* sp. AD-3-6 described herein provides the first direct support of **3** as a probable biosynthetic intermediate. Subsequent NybT/U-catalyzed isopenicillin N synthase-like ring closure was proposed to afford hypothetical intermediate

III, followed by NybB-catalyzed C-12 hydroxylation to **4**. Within this context, additional C-12 oxidation of **4** would yield **1**, one of the major pyridoquinolinedione-based metabolites isolated in the current study. The isolation of metabolites **2** and **5**, both lacking the methylene bridge, suggests a central C-14 oxidative demethylation step potentially originating from putative intermediate III. As a chemical precedent, previously reported chemical degradation of a semisynthetic intermediate III using MnO₂ yielded intermediate IV.⁷⁶ Following demethylation, intermediate IV could be hydroxylated by NybB to give **2**, oxidized to the *p*-quinone **5**, or glycosylated to form pseudonocardin C, the latter two of which are previously reported metabolites of *Pseudonocardia* sp. SCSIO 01299.⁴³ Metabolite **5** could also serve as the precursor for pseudonocardins A and B, wherein the pyrrolidine ring may surprisingly reflect an artifact due to metabolite isolation via acetone or 2-butanone extraction. Consistent with this hypotheses, incubation of **5** in the presence of acetone (Supporting Information, Figure S36), followed by LC-MS analysis, gave a product with a UV/vis and MS signature consistent with that of pseudonocardin A. Cumulatively, the new metabolites and concepts resulting from this study are anticipated to enable future biochemical studies that support or refute the proposed biosynthetic hypotheses highlighted above.

MATERIALS AND METHODS

General Experimental Procedures.

UV spectra were recorded on an Ultrospec 8000 spectrometer (GE, Pittsburgh, PA, USA). All NMR spectra were recorded at 400 MHz for ¹H and 100 MHz for ¹³C with Varian Inova NMR spectrometers (Agilent, Santa Clara, CA, USA). HPLC-MS was conducted with an Agilent 6120 quadrupole MSD mass spectrometer (Agilent Technologies, Santa Clara, CA, USA) equipped with an Agilent 1200 series quaternary LC system and an Eclipse XDB-C18 column (150 × 4.6 mm, 5 μm). HR-ESI-MS spectra were recorded on an AB SCIEX Triple TOF 5600 system (AB Sciex, Framingham, MA, USA). HPLC analyses were performed on an Agilent 1260 system equipped with a photodiode array (PDA) detector and a Phenomenex C₁₈ column (250 × 4.6 mm, 5 μm; Phenomenex, Torrance, CA). Semipreparative HPLC separation was performed on a Varian Prostar 210 HPLC system equipped with a PDA detector using a Supelco DiscoveryBio wide pore C18 column (250 × 21.2 mm, 10 μm; flow rate, 8 mL/min; Sigma-Aldrich, St. Louis, MO, USA). Size exclusion chromatography was performed on Sephadex LH-20 (25–100 μm; GE Healthcare, Piscataway, NJ, USA). Amberlite XAD16N resin (20–60 mesh) was purchased from Sigma-Aldrich (St. Louis, MO, USA). TLC silica gel plates (60 F₂₅₄) were purchased from EMD Chemicals Inc. (Darmstadt, Germany). *Staphylococcus aureus*, *Bacillus subtilis*, *Salmonella enterica*, *Mycobacterium aurum*, and *Saccharomyces cerevisiae* strains and human cancer cell lines A549 (ATCC CCL185 human lung non-small cell carcinoma), HCT116 (ATCC CCL-247 human colorectal carcinoma), and PC3 (ATCC CRL1435 human prostate adenocarcinoma) were obtained from ATCC (Manassas, VA, USA). *Micrococcus luteus* and *Escherichia coli* strains were obtained from NRRL (Peoria, IL, USA). All solvents used were of ACS grade and purchased from the Pharmco-AAPER (Brookfield, CT, USA). All other reagents used were reagent grade and purchased from Sigma-Aldrich (St. Louis, MO, USA).

Isolation and Identification of *Streptomyces* sp. AD-3-6.

The soil sample was collected from an acid mine drainage site in McCreary County, KY (GPS coordinates: 36°42'03.4"N 84°34'04.7"W). Metabolic profiling and strain isolation followed previously reported protocols.^{19,20,22} Strain identification, based on 16S rRNA sequencing following previously described protocols,^{26,27} revealed 99% identity (BLAST search) with the 16S rRNA gene sequence of *Streptomyces iakyrus* strain NBRC 13401. The sequence of 16S rRNA has been deposited in the NCBI nucleotide database with the accession number KX902490.

Scale-up Fermentation.

Streptomyces sp. AD-3-6 was cultivated in three 250 mL Erlenmeyer flasks, each containing 50 mL of medium A (soluble starch, 20.0 g/L; glucose, 10.0 g/L; peptone, 5.0 g/L; yeast extract, 5.0 g/L; NaCl, 4.0 g/L; K₂HPO₄, 0.5 g/L; MgSO₄·7H₂O, 0.5 g/L; CaCO₃, 2.0 g/L, pH 7.0). After 3 days of incubation at 28 °C with 200 rpm agitation, the cultures were used to inoculate 100 flasks (250 mL), each containing 100 mL of medium A (total 10 L). The fermentation was continued for 10 days at 28 °C with 200 rpm agitation. The combined culture broth was centrifuged at 3000g for 30 min (4 °C) to provide the solid biomass and supernatant. The cumulative biomass (mycelium) was extracted with MeOH (3 × 600 mL), and the corresponding recovered organics were subsequently evaporated in vacuo at 40 °C to yield 15.3 g of crude extract. The supernatant was mixed with 3% (w/v) XAD-16 resin and stirred overnight, followed by filtration. The resin was washed with H₂O (3 × 600 mL) and then extracted with MeOH until the eluant was colorless. The combined MeOH extracts were subsequently evaporated to afford 10.8 g of crude extract. Both extracts (obtained from the biomass and supernatant) revealed a similar metabolite profile based on HPLC and TLC analyses and were therefore combined.

As highlighted in Scheme S1, the combined crude extract (26.1 g) was subjected to HP-20SS resin column chromatography (800g, 40 × 8 cm) eluted with a gradient of aqueous MeOH (20–100%) to yield five fractions (A–E). Fraction B (1.5 g) was resolved by size-exclusion chromatography (Sephadex LH-20, 4 × 100 cm, 2 mL/min, MeOH) to yield three subfractions, B1–B3 (100 mL each). Subfraction B2 (0.3 g) was further purified by a semipreparative HPLC (10–30% CH₃CN/0.025% TFA over 30 min) to afford compound **1** (15.0 mg, white amorphous powder, retention time: 11.8 min). Fraction C (1.3 g) was subjected to Sephadex LH-20 column (4 × 100 cm, 2 mL/min, MeOH) and the recovered subfraction C2 (0.2 g) further purified by a semipreparative HPLC (5–40% CH₃CN/0.025% TFA over 30 min) to yield compounds **2** (5.0 mg, white amorphous powder, retention time: 10.1 min) and **9** [2-(1,3-pentadien-1-yl)-4-piperidinol, 6.0 mg, white amorphous powder, retention time: 13.4 min]. Fraction D (2.7 g) was subjected to Sephadex LH-20 column chromatography (4 × 100 cm, 2 mL/min, MeOH) to yield three subfractions, D1–D3 (120 mL each). Subfraction D2 (0.8 g) was further purified by a semipreparative HPLC (20–45% CH₃CN/0.025% TFA over 25 min) to yield compounds **3** (3.0 mg, white amorphous powder, retention time: 14.5 min), **5** (2.0 mg, white amorphous powder, retention time: 13.4 min), and **4** (25.0 mg, white amorphous powder, retention time: 12.0 min). Fraction E (2.4 g) was subjected to a silica gel column (50 g, 12 × 4 cm) eluted with CHCl₃/MeOH (10:0–1:1) to yield five fractions, E1–E5. Subfraction E5 (0.3 g) was further purified by semipreparative

HPLC (45–75% CH₃CN/0.05% TFA over 30 min) to afford compound **6** (2.0 mg, red amorphous powder, retention time: 21.6 min). Subfraction E3 (0.4 g) was further purified by semipreparative HPLC (50–70% CH₃CN/0.05% TFA over 25 min) to afford compounds **7** (11.0 mg, red amorphous powder, retention time: 21.0 min) and **8** (6.0 mg, red amorphous powder, retention time: 24.1 min).

Nybomycin B (1): white amorphous powder; UV (DMSO) λ_{\max} (log ϵ) 273 (9.27), 294 (8.04), 379 (3.66) nm; for ¹³C and ¹H NMR data, see Table 1; (+)-ESI-MS m/z 313.0 [M + H]⁺; (+)-HR-ESI-MS m/z 313.0820 [M + H]⁺ (calcd for C₁₆H₁₃N₂O₅, 313.0824).

Nybomycin C (2): white amorphous powder; UV (DMSO) λ_{\max} (log ϵ) 284 (15.37), 357 (4.77), 375 (5.57) nm; for ¹³C and ¹H NMR data, see Table 1; (+)-ESI-MS m/z 287.0 [M + H]⁺, (–)-ESI-MS m/z 285.0 [M – H][–]; (+)-HR-ESI-MS m/z 287.1030 [M + H]⁺ (calcd for C₁₅H₁₅N₂O₄, 287.1032).

Nybomycin D (3): white amorphous powder; UV (DMSO) λ_{\max} (log ϵ) 290 (14.44), 359 (3.61), 376 (3.67) nm; for ¹³C and ¹H NMR data, see Table 1; (+)-ESI-MS m/z 285.1 [M + H]⁺, (–)-ESI-MS m/z 283.0 [M – H][–]; (+)-HR-ESI-MS m/z 285.1240 [M + H]⁺ (calcd for C₁₆H₁₇N₂O₃, 285.1239).

Antibacterial, Antifungal, and Cancer Cell Line Viability Assays.

Antibacterial (*Staphylococcus aureus* ATCC 6538, *Micrococcus luteus* ATCC 15307, *Bacillus subtilis* ATCC 6633, *Mycobacterium aurum* ATCC 23366, *Escherichia coli* ATCC 12435, and *Salmonella enterica* ATCC 10708), antifungal (*Saccharomyces cerevisiae* ATCC 204508), and cytotoxicity (human non-small cell lung cancer cell A549 and prostate cancer cell PC3) assays were accomplished in triplicate following our previously reported protocols.^{20,77} Antibacterial/antifungal MIC values were obtained after 16–48 h incubation. Vehicle (DMSO) was used as the negative control, and kanamycin and ampicillin (*S. aureus*, *M. luteus*, *B. subtilis*, *M. aurum*, *S. enterica*, and *E. coli*), amphotericin B (*S. cerevisiae*), and actinomycin D (A549 and PC3) were used as positive controls.

Axolotl Embryo Tail Regeneration Assay.

The axolotl embryo tail regeneration assay was conducted following our previously reported protocols.^{25,27,30,32,33} Axolotls (RRID:AGSC_100E) were obtained from the Ambystoma Genetic Stock Center (RRID:SCR_006372). Vehicle (DMSO) was used as the negative control, and the Hsp90 inhibitor geldanamycin was used as a positive control.

Western Blot Analysis.

Western blot analysis was performed as previously described.^{29,30}

Supplementary Material

Refer to Web version on PubMed Central for supplementary material.

ACKNOWLEDGMENTS

This work was supported by National Institutes of Health Grant Nos. R24 OD21479 (S.R.V., J.S.T.), R01 CA203257 (Q.B.S., J.S.T.), R01 CA175105 (Q.B.S.), and R01 GM115261 (J.S.T.), the University of Kentucky College of Pharmacy, the University of Kentucky Markey Cancer Center, and the National Center for Advancing Translational Sciences (UL1TR000117 and UL1TR001998). We thank the College of Pharmacy NMR Center (University of Kentucky) for NMR support.

REFERENCES

- (1). Strelitz F; Flon H; Asheshov IN Proc. Natl. Acad. Sci. U. S. A 1955, 41, 620–624. [PubMed: 16589716]
- (2). Eble TE; Boyack GA; Large CM; Devries WH Antibiot. Chemother 1958, 8, 627–630.
- (3). Arai M; Kamiya K; Pruksakorn P; Sumii Y; Kotoku N; Joubert JP; Moodley P; Han C; Shin D; Kobayashi M Bioorg. Med. Chem 2015, 23, 3534–3541. [PubMed: 25934225]
- (4). Rodríguez Estévez M; Myronovskyi M; Gummerlich N; Nadmid S; Luzhetskyy A Mar. Drugs 2018, 16, 435.
- (5). Zakalyukina YV; Birykov MV; Lukianov DA; Shiriaev DI ; Komarova ES; Skvortsov DA; Kostyukevich Y; Tashlitsky VN; Polshakov VI; Nikolaev E; Sergiev PV; Osterman IA Biochimie 2019, 160, 93–99. [PubMed: 30797881]
- (6). Hiramatsu K; Igarashi M; Morimoto Y; Baba T; Umekita M; Akamatsu Y Int. J. Antimicrob. Agents 2012, 39, 478–485. [PubMed: 22534508]
- (7). Parkinson EI; Bair JS; Nakamura BA; Lee HY; Kuttub HI; Southgate EH; Lezmi S; Lau GW; Hergenrother P Nat. Commun 2015, 6, 6947. [PubMed: 25907309]
- (8). Morimoto Y; Baba T; Sasaki T; Hiramatsu K Int. J. Antimicrob. Agents 2015, 46, 666–673. [PubMed: 26526895]
- (9). Bair JS; Palchaudhuri R; Hergenrother PJ J. Am. Chem. Soc 2010, 132, 5469–5478. [PubMed: 20345134]
- (10). Parkinson EI; Hergenrother PJ Acc. Chem. Res 2015, 48, 2715–2723. [PubMed: 26444384]
- (11). Ponnuraj N; Kolossov V; Parkinson E; Benefiel A; Hergenrother P; Gaskins H FASEB J. 2014, 28, 655.10.
- (12). Lee HY; Parkinson EI; Granchi C; Paterni I; Panigrahy D; Seth P; Minutolo F; Hergenrother PJ ACS Chem. Biol 2017, 12, 1416–1424. [PubMed: 28345875]
- (13). Parkinson EI; Bair JS; Cismesia M; Hergenrother PJ ACS Chem. Biol 2013, 8, 2173–2183. [PubMed: 23937670]
- (14). Huang X; Dong Y; Bey EA; Kilgore JA; Bair JS; Li LS; Patel M; Parkinson EI; Wang Y; Williams NS; Gao J; Hergenrother PJ; Boothman DA Cancer Res. 2012, 72, 3038–3047. [PubMed: 22532167]
- (15). Nussbaum F; Ebbinghaus A; Mayer-Bartschmid A; Zitzmann W; Wiese W-B; Stadler M; Anlauf S CDC25 inhibitors. Patent Appl. EP2130831A1, 2009.
- (16). Sur S; Agrawal DK Mol. Cell. Biochem 2016, 416, 33–46. [PubMed: 27038604]
- (17). Nadzan AM; Rinehart KL Jr. J. Am. Chem. Soc 1976, 98, 5012–5014. [PubMed: 950425]
- (18). Nadzan AM; Rinehart KL Jr. J. Am. Chem. Soc 1977, 99, 4647–4654. [PubMed: 874227]
- (19). Shaaban KA; Wang X; Elshahawi SI; Ponomareva LV; Sunkara M; Copley GC; Hower JC; Morris AJ; Kharel MK; Thorson JS J. Nat. Prod 2013, 76, 1619–1626. [PubMed: 23947794]
- (20). Wang X; Shaaban KA; Elshahawi SI; Ponomareva LV; Sunkara M; Zhang Y; Copley GC; Hower JC; Morris AJ; Kharel MK; Thorson JS J. Nat. Prod 2013, 76, 1441–1447. [PubMed: 23944931]
- (21). Wang X; Elshahawi SI; Shaaban KA; Fang L; Ponomareva LV; Zhang Y; Copley GC; Hower JC; Zhan CG; Kharel MK; Thorson JS Org. Lett 2014, 16, 456–459. [PubMed: 24341358]
- (22). Wang X; Shaaban KA; Elshahawi SI; Ponomareva LV; Sunkara M; Copley GC; Hower JC; Morris AJ; Kharel MK; Thorson JS J. Antibiot 2014, 67, 571–575. [PubMed: 24713874]

- (23). Wang X; Reynolds AR; Elshahawi SI; Shaaban KA; Ponomareva LV; Saunders MA; Elgumati IS; Zhang Y; Copley GC; Hower JC; Sunkara M; Morris AJ; Kharel MK; Van Lanen SG; Prendergast MA; Thorson JS *Org. Lett* 2015, 17, 2796–2799. [PubMed: 25961722]
- (24). Shaaban KA; Saunders MA; Zhang Y; Tran T; Elshahawi SI; Ponomareva LV; Wang X; Zhang J; Copley GC; Sunkara M; Kharel MK; Morris AJ; Hower JC; Tremblay MS; Prendergast MA; Thorson JS *J. Nat. Prod* 2017, 80, 2–11. [PubMed: 28029795]
- (25). Wang X; Zhang Y; Ponomareva LV; Qiu Q; Woodcock R; Elshahawi SI; Chen X; Zhou Z; Hatcher BE; Hower JC; Zhan CG; Parkin S; Kharel MK; Voss SR; Shaaban KA; Thorson JS *Angew. Chem. Int. Ed* 2017, 56, 2994–2998.
- (26). Abbas M; Elshahawi SI; Wang X; Ponomareva LV; Sajid I; Shaaban KA; Thorson JS *J. Nat. Prod* 2018, 81, 2560–2566. [PubMed: 30418763]
- (27). Wang X; Abbas M; Zhang Y; Elshahawi SI; Ponomareva LV; Cui Z; Van Lanen SG; Sajid I; Voss SR; Shaaban KA; Thorson JS *J. Nat. Prod* 2019, 82, 1686–1693. [PubMed: 31117525]
- (28). Fatima A; Aftab U; Shaaban KA; Thorson JS; Sajid I *BMC Microbiol.* 2019, 19 (1), 49. [PubMed: 30795744]
- (29). Ye Q; Zhang Y; Cao Y; Wang X; Guo Y; Chen J; Horn J; Ponomareva LV; Chaiswing L; Shaaban KA; Wei Q; Anderson BD; St Clair DK; Zhu H; Leggas M; Thorson JS; She QB *Cell. Chem. Biol* 2019, 26, 366–377. [PubMed: 30661989]
- (30). Zhang Y; Ye Q; Ponomareva LV; Cao Y; Liu Y; Cui Z; Van Lanen SG; Voss SR; She QB; Thorson JS *Chem. Sci* 2019, 10, 7641–7648. [PubMed: 31583069]
- (31). Elshahawi SI; Cao H; Shaaban KA; Ponomareva LV; Subramanian T; Farman ML; Spielmann HP; Phillips GN Jr.; Thorson JS; Singh S *Nat. Chem. Biol* 2017, 13, 366–368. [PubMed: 28166207]
- (32). Ponomareva LV; Athipozhy A; Thorson JS; Voss SR *Comp. Biochem. Physiol., Part C: Toxicol. Pharmacol* 2015, 178, 128–135.
- (33). Voss SR; Ponomareva LV; Dwaraka VB; Pardue KE; Baddar N; Rodgers AK; Woodcock MR; Qiu Q; Crowner A; Blichmann D; Khatri S; Thorson JS *Sci. Rep* 2019, 9, 6751. [PubMed: 31043677]
- (34). Laatsch H *AntiBase 2017*; Wiley-VCH: Weinheim, Germany, 2017.
- (35). Rinehart KL Jr.; Leadbetter G; Larson RA; Forbis RM *J. Am. Chem. Soc* 1970, 92, 6994–6995. [PubMed: 5483074]
- (36). Forbis RM; Rinehart KL Jr. *J. Am. Chem. Soc* 1970, 92, 6995–6996. [PubMed: 5483075]
- (37). Naganawa H; Wakashiro T; Yagi A; Kondo S; Takita T; Hamada M; Maeda K; Umezawa H *J. Antibiot.* 1970, 23, 365–368. [PubMed: 5460278]
- (38). Brockmann H; Lenk W; Schwantje G; Zeeck A *Tetrahedron Lett.* 1966, 7, 3525–3530.
- (39). Puder C; Loya S; Hizi A; Zeeck A *Eur. J. Org. Chem* 2000, 2000, 729–735.
- (40). Akai S; Kakiguchi K; Nakamura Y; Kuriwaki I; Dohi T; Harada S; Kubo O; Morita N; Kita Y *Angew. Chem. Int. Ed* 2007, 46, 7458–7461.
- (41). Grabley S; Hammann P; Kluge H; Wink J; Kricke P; Zeeck A *J. Antibiot.* 1991, 44, 797–800. [PubMed: 1880070]
- (42). Nadzan AM; Rinehart KL Jr.; Sokolski WT *J. Antibiot* 1977, 30, 523–524. [PubMed: 885812]
- (43). Li S; Tian X; Niu S; Zhang W; Chen Y; Zhang H; Yang X; Zhang W; Li W; Zhang S; Ju J; Zhang C *Mar. Drugs* 2011, 9, 1428–1439. [PubMed: 21892356]
- (44). Ojiri K; Suda H; Okura A; Kawamura K; Okanishi M *Anticancer agent BE-12233 manufacture with Streptomyces. Patent Appl. JP 03030688 A2*, 1991.
- (45). Chu M; Mierzwa R; Xu L; Yang SW; He L; Patel M; Stafford J; Macinga D; Black T; Chan TM; Gullo V *Bioorg. Med. Chem. Lett* 2003, 13, 3827–3829. [PubMed: 14552789]
- (46). Pettit GR; Du J; Pettit RK; Richert LA; Hogan F; Mukku VJ; Hoard MS *J. Nat. Prod* 2006, 69, 804–806. [PubMed: 16724845]
- (47). Murata M; Miyasaka T; Tanaka H; Omura S *J. Antibiot* 1985, 38, 1025–1033. [PubMed: 3840154]
- (48). Maskey RP; Grün-Wollny I; Laatsch H *Nat. Prod. Res* 2005, 19, 137–142. [PubMed: 15715257]

- (49). Omura S; Iwai Y; Hinotozawa K; Tanaka H; Takahashi Y; Nakagawa A J. *Antibiot.* 1982, 35, 1425–1429. [PubMed: 7161180]
- (50). Mullowney M; O'hAinmhire E; Shaikh A; Wei X; Tanouye U; Santarsiero B; Burdette J; Murphy B *Mar. Drugs* 2014, 12, 3574–3586. [PubMed: 24921978]
- (51). Prior AM; Sun D *RSC Adv.* 2019, 9, 1759–1771.
- (52). Mullowney MW; Hwang CH; Newsome AG; Wei X; Tanouye U; Wan B; Carlson S; Barranis NJ; Ó hAinmhire E; Chen W-L; Krishnamoorthy K; White J; Blair R; Lee H; Burdette JE; Rathod PK; Parish T; Cho S; Franzblau SG; Murphy BT *ACS Infect. Dis* 2015, 1, 168–174. [PubMed: 26594660]
- (53). Bhat M; Robichaud N; Hulea L; Sonenberg N; Pelletier J; Topisirovic I *Nat. Rev. Drug Discovery* 2015, 14, 261–278. [PubMed: 25743081]
- (54). BousseSMART L; Malka-Mahieu H; Girault I; Allard D; Hemmingsson O; Tomasic G; Thomas M; Basmadjian C; Ribeiro N; Thuaud F; Mateus C; Routier E; Kamsu-Kom N; Agoussi S; Eggermont AM; Desaubry L; Robert C; Vagner S *Nature* 2014, 513, 105–109. [PubMed: 25079330]
- (55). Cai W; Ye Q; She QB *Oncotarget* 2014, 5, 6015–6027. [PubMed: 24970798]
- (56). Ducker GS; Atreya CE; Simko JP; Hom YK; Matli MR; Benes CH; Hann B; Nakakura EK; Bergsland EK; Donner DB; Settleman J; Shokat KM; Warren RS. *Oncogene* 2014, 33, 1590–1600. [PubMed: 23542178]
- (57). Hsieh AC; Costa M; Zollo O; Davis C; Feldman ME; Testa JR; Meyuhas O; Shokat KM; Ruggero D *Cancer Cell* 2010, 17, 249–261. [PubMed: 20227039]
- (58). Mi W; Ye Q; Liu S; She QB *Oncotarget* 2015, 6, 13962–13977. [PubMed: 25961827]
- (59). She QB; Halilovic E; Ye Q; Zhen W; Shirasawa S; Sasazuki T; Solit DB; Rosen N *Cancer Cell* 2010, 18, 39–51. [PubMed: 20609351]
- (60). Ye Q; Cai W; Zheng Y; Evers BM; She QB *Oncogene* 2014, 33, 1828–1839. [PubMed: 23624914]
- (61). Zhang J; Kim J; Alexander A; Cai S; Tripathi DN; Dere R; Tee AR; Tait-Mulder J; Di Nardo A; Han JM; Kwiatkowski E ; Dunlop EA; Dodd KM; Folkert RD; Faust PL; Kastan MB; Sahin M; Walker CL *Nat. Cell Biol* 2013, 15, 1186–1196. [PubMed: 23955302]
- (62). Chen MF; Keng PC; Shau H; Wu CT; Hu YC; Liao SK; Chen WC *Int. J. Radiat. Oncol., Biol., Phys* 2006, 64, 581–591. [PubMed: 16414373]
- (63). Ueno T; Takahashi H; Oda M; Mizunuma M; Yokoyama A; Goto Y; Mizushima Y; Sakaguchi K; Hayashi H *Biochemistry* 2000, 39, 5995–6002. [PubMed: 10821671]
- (64). Goldman ME; Salituro GS; Bowen JA; Williamson JM; Zink DL; Schleif WA; Emini EA *Mol. Pharmacol* 1990, 38, 20–25. [PubMed: 1695317]
- (65). Bernardo CE; Silva PJ *PeerJ* 2014, 2, e470. [PubMed: 25071993]
- (66). Atkinson DJ; Brimble MA *Nat. Prod. Rep* 2015, 32, 811–840. [PubMed: 25798711]
- (67). Cohn EP; Wu KL; Pettus TR; Reich NO *J. Med. Chem* 2012, 55, 3678–3686. [PubMed: 22413845]
- (68). Mizushima Y; Takeuchi T; Sugawara F; Yoshida H *Mini-Rev. Med. Chem* 2012, 12, 1135–1143. [PubMed: 22876944]
- (69). Chen JL-Y; Sperry J; Ip NY; Brimble MA *MedChemComm* 2011, 2, 229–245.
- (70). West MD; Sternberg H; Labat I; Janus J; Chapman KB; Malik NN; de Grey AD; Larocca D *Regener. Med* 2019, 14, 867–886.
- (71). Godic A *Clin. Dermatol* 2019, 37, 320–325. [PubMed: 31345319]
- (72). Kumar M; Lechel A; Gunes C *Genes* 2016, 7, 43.
- (73). Carneiro MC; de Castro IP; Ferreira MG *Dis. Models & Mech* 2016, 9, 737–748.
- (74). Wu RA; Upton HE; Vogan JM; Collins K *Annu. Rev. Biochem* 2017, 86, 439–460. [PubMed: 28141967]
- (75). Alibardi LJ. *Exp. Zool, Part A* 2015, 323, 757–766.
- (76). Knoll WM; Huxtable RJ; Rinehart KL Jr. *J. Am. Chem. Soc* 1973, 95, 2703–2704. [PubMed: 4694531]

- (77). Shaaban KA; Elshahawi SI; Wang X; Horn J; Kharel MK; Leggas M; Thorson JS J. *Nat. Prod* 2015, 78, 1723–1729. [PubMed: 26091285]

Author Manuscript

Author Manuscript

Author Manuscript

Author Manuscript

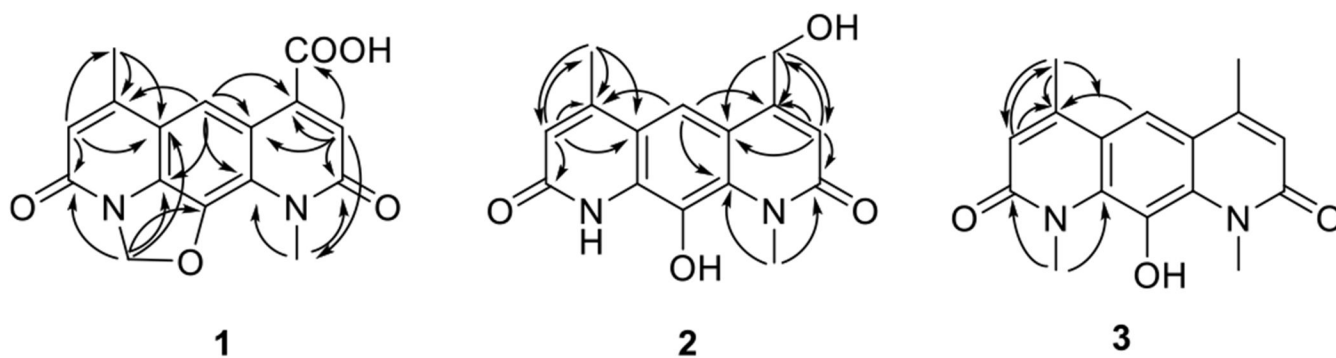


Figure 1.
Selected HMBC (\rightarrow) correlations of nybomycins B–D (1–3).

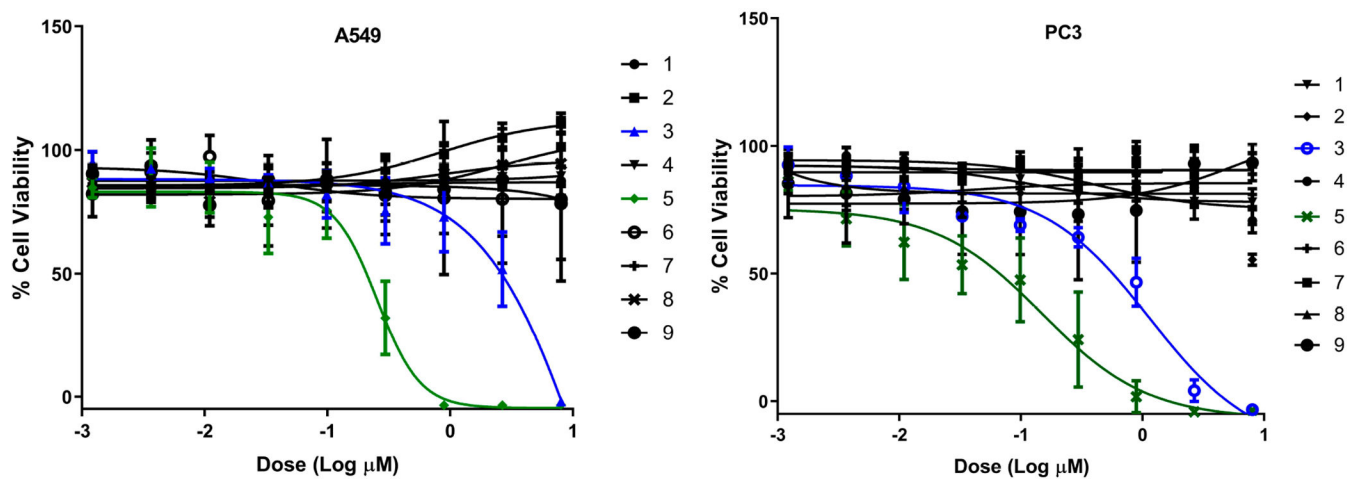


Figure 2.
Dose–response of compounds **1–9** against A549 (non-small cell lung) and PC3 (prostate) human cancer cell lines (72 h). For EC_{50} values, see Table 2.

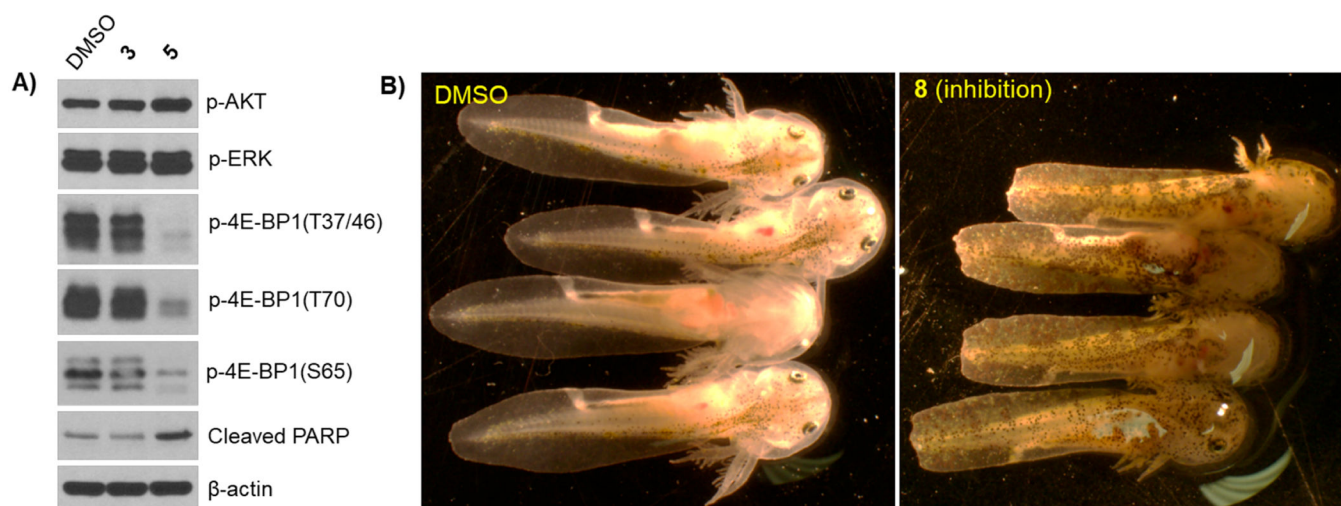


Figure 3.

(A) HCT116 cells were treated with 2 μM **3** and 1 μM **5** or DMSO (negative control) for 6 h followed by Western blot analysis for the indicated proteins. (B) Impact of 1 μM **8** on axolotl embryo tail regeneration at 7 dpa compared to vehicle control (DMSO). Note that control embryos but not embryos treated with **8** regenerated a rounded tail tip typical of the unamputated condition.

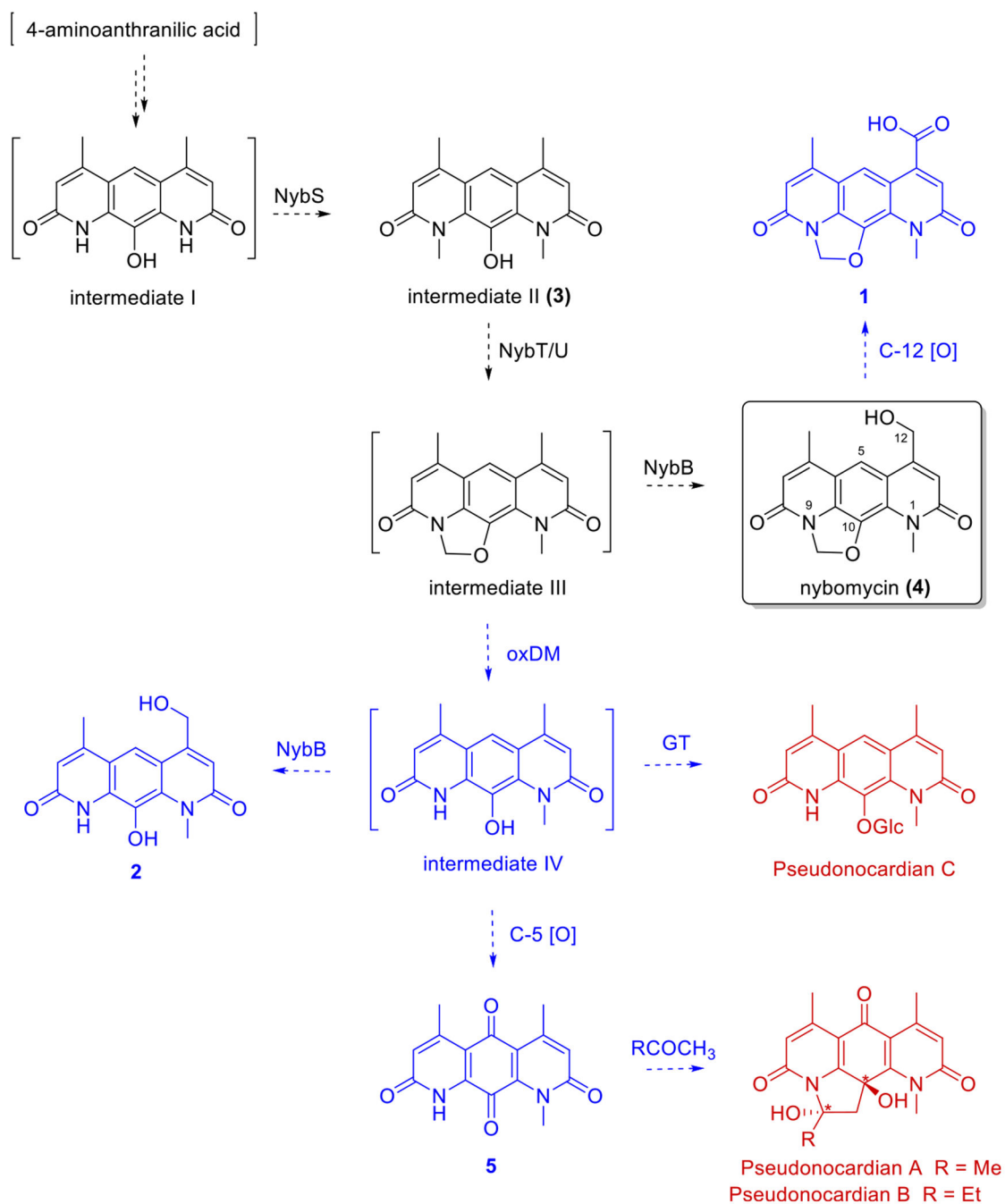


Figure 4. *Streptomyces* sp. AD-3-6-derived nybomycins **2–5** within the context of the biosynthetic pathway put forth by Luzhetskyy and colleagues (black) and pseudocardians previously reported by Zhang et al. (red; *only relative stereochemistry assigned). Proposed biosynthetic revisions based on the current study are highlighted (blue). Compounds in brackets are putative intermediates, and dashed arrows represent putative transformations with possible enzyme catalysts noted where possible. Metabolite **3** reported herein was

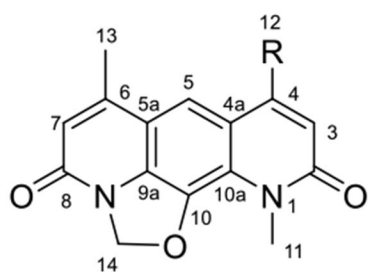
previously proposed by Luzhetskyy et al. as a biosynthetic intermediate, whereas metabolite **5** and pseudonocardians were previously reported by Zhang et al.

Author Manuscript

Author Manuscript

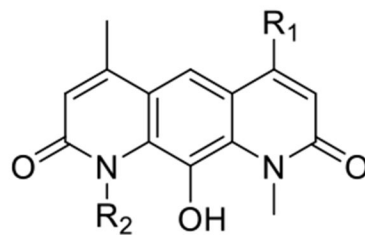
Author Manuscript

Author Manuscript



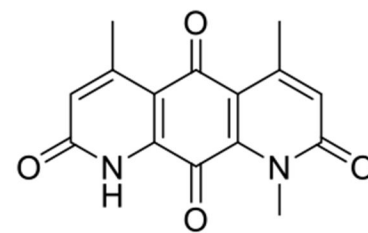
1: R = COOH

4: R = CH₂OH

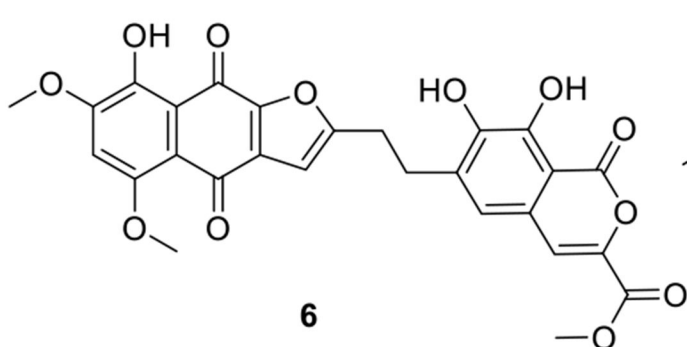


2: R₁ = CH₂OH, R₂ = H

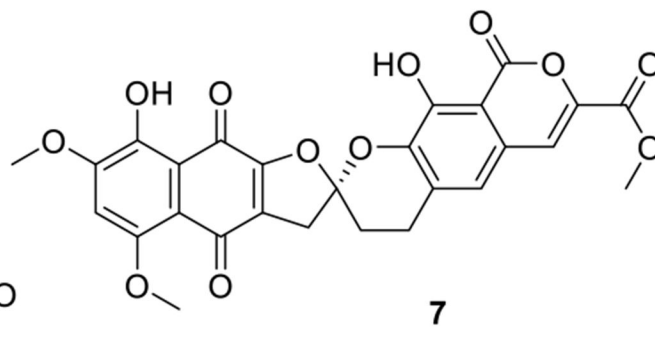
3: R₁ = CH₃, R₂ = CH₃



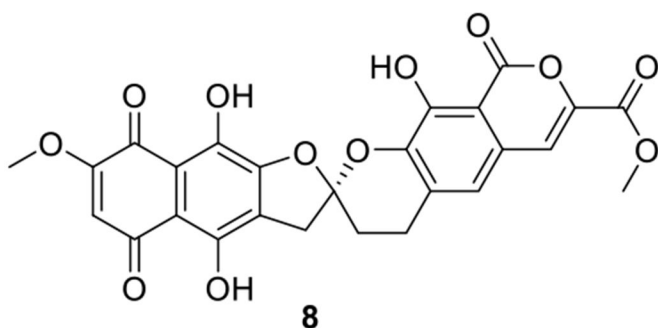
5



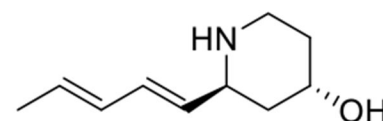
6



7



8



9

Chart 1.

^{13}C (100 MHz) and ^1H (400 MHz) NMR Spectroscopic Data of Nybomycins B–D (1–3) and Nybomycin 4 in CF_3COOD

Table 1.

| no. | nybomycin B (1) | | nybomycin C (2) | | nybomycin D (3) | | nybomycin (4) | |
|-----|----------------------------|-----------------------------|----------------------------|-----------------------------|----------------------------|-----------------------------|----------------------------|-----------------------------|
| | δ_{C} , type | δ_{H} , mult. | δ_{C} , type | δ_{H} , mult. | δ_{C} , type | δ_{H} , mult. | δ_{C} , type | δ_{H} , mult. |
| 2 | 163.3, C | | 163.8, C | | 164.8, C | | 162.8, C | |
| 3 | 122.5, CH | 7.47, s | 116.2, CH | 7.42, s | 115.1, CH | 7.30, s | 110.3, CH | 7.30, s |
| 4 | 140.2, C | | 146.5, C | | 156.3, C | | 155.0, C | |
| 4a | 118.8, C | | 119.0, C | | 123.2, C | | 119.0, C | |
| 5 | 116.7, CH | 8.59, s | 115.9, CH | 8.35, s | 116.5, CH | 8.41, s | 111.9, CH | 8.41, s |
| 5a | 117.1, C | | 120.1, C | | 123.2, C | | 116.4, C | |
| 6 | 155.0, C | | 156.8, C | | 156.3, C | | 151.3, C | |
| 7 | 117.8, CH | 6.78, s | 116.4, CH | | 115.1, CH | | 119.2, CH | |
| 8 | 160.0, C | | 162.7, C | | 164.8, C | | 159.4, C | |
| 9a | 130.9, C | | 132.1, C | | 136.9, C | | 131.1, C | |
| 10 | 138.2, C | | 132.2, C | | 133.6, C | | 137.8, C | |
| 10a | 124.7, C | | 131.8, C | | 136.9, C | | 122.4, C | |
| 11 | 33.8, CH_3 | 4.01, s | 36.0, CH_3 | 4.43, s | 38.4, CH_3 | 4.37, s | 33.4, CH_3 | 4.09, s |
| 12 | 169.0, C | | 64.3, CH_2 | 5.99, s | 17.8, CH_3 | 2.86, s | 59.4, CH_3 | 5.09, s |
| 13 | 16.2, CH_3 | 2.49, s | 17.5, CH_3 | 2.91, s | 17.8, CH_3 | 2.86, s | 15.5, CH_3 | 2.50, s |
| 14 | 86.8, CH_2 | 6.42, s | | | 38.4, CH_3 | 4.37, s | 85.9, CH_2 | 6.42, s |

Table 2.

Antimicrobial and Cytotoxic Activities of Compounds 1–9^a

| compounds | MIC μM ($\mu\text{g/mL}$) | | | | | | | | | EC ₅₀ μM | | |
|-----------|--|------------------|--------------------|-----------------|----------------|--------------------|----------------------|-------|------|--------------------------------|--|--|
| | <i>S. aureus</i> | <i>M. luteus</i> | <i>B. subtilis</i> | <i>M. aurum</i> | <i>E. coli</i> | <i>S. enterica</i> | <i>S. cerevisiae</i> | A549 | PC3 | | | |
| 1 | >24 (7.5) | >24 (7.5) | >24 (7.5) | >24 (7.5) | >24 (7.5) | >24 (7.5) | >24 (7.5) | >100 | >100 | >100 | | |
| 2 | >24 (6.9) | >24 (6.9) | >24 (6.9) | >24 (6.9) | >24 (6.9) | >24 (6.9) | >24 (6.9) | >100 | >100 | >100 | | |
| 3 | 12 (3.4) | 12 (3.4) | 6 (1.7) | >24 (6.8) | >24 (6.8) | >24 (6.8) | >24 (6.8) | 15.17 | 1.14 | >100 | | |
| 4 | >24 (7.2) | 12 (3.6) | 12 (3.6) | >24 (7.2) | >24 (7.2) | >24 (7.2) | >24 (7.2) | >100 | >100 | >100 | | |
| 5 | 12 (3.4) | 12 (3.4) | 12 (3.4) | >24 (6.8) | >24 (6.8) | >24 (6.8) | >24 (6.8) | 0.25 | 0.15 | >100 | | |
| 6 | 3 (1.6) | 1.5 (0.8) | 0.4 (0.2) | >24 (12.9) | >24 (12.9) | >24 (12.9) | >24 (12.9) | >100 | >100 | >100 | | |
| 7 | 12 (6.4) | 6 (3.2) | 12 (6.4) | >24 (12.9) | >24 (12.9) | >24 (12.9) | 12 (6.4) | >100 | >100 | >100 | | |
| 8 | 0.075 (0.04) | 0.15 (0.08) | 0.02 (0.01) | 12 (6.3) | >24 (12.6) | >24 (12.6) | 3 (1.6) | >100 | >100 | >100 | | |
| 9 | >24 (4.0) | >24 (4.0) | >24 (4.0) | >24 (4.0) | >24 (4.0) | >24 (4.0) | >24 (4.0) | >100 | >100 | >100 | | |

^a Antibacterial/antifungal MIC values were obtained after 16–48 h incubation. Kanamycin [*S. aureus*, 7.5 (4); *M. luteus*, 15 (9); *B. subtilis*, 2 (1); *S. enterica*, 14 (8); and *E. coli* 7.5 (4)]. Ampicillin [*S. aureus*, 12 (4); *M. luteus*, 25 (9); *S. enterica*, 25 (9); and *E. coli* 25 (9)] rifampicin [*M. aurum*, 2 (1)], amphotericin B [*S. cerevisiae*, 2 (1)] were used as positive controls. Cytotoxicity EC₅₀/IC₅₀ values were obtained after 72 h incubation. Actinomycin D and H₂O₂ [A549 (non-small cell lung), PC3 (prostate) human cancer cell lines] were used as positive control at 20 μM and 2 mM concentration, respectively (0% viable cells).